MICROARRAY DETECTION OF GENE OVEREXPRESSION IN PRIMARY SPONTANEOUS PNEUMOTHORAX

Journal:	*Experimental Lung Research*
Manuscript ID:	UELR-2009-0088.R2
Manuscript Type:	Original Papers
Date Submitted by the Author:	
Complete List of Authors:	Fang, Hsin-Yuan; China Medical University Hospital, China Medical University, Thoracic Surgery Ching-Yuang, Lin; China Medical University Hospital Chow, Kuan-Chih; National Chung Hsing University, Graduate Institutes of Biomedical Sciences Huang, Hung-Che; Changhua Christian Hospital, Surgery Ko, Wen-Je; National Taiwan University Hospital, Surgery
Keywords:	primary spontaneous pneumothorax, gene expression, microarray, hypoxia, HIF-3a, caspase-8

MICROARRAY DETECTION OF GENE OVEREXPRESSION IN PRIMARY SPONTANEOUS PNEUMOTHORAX

Running head: Gene overexpression and PSP

Hsin-Yuan Fang, M.D.[a,b], Ching-Yuang Lin, M.D., Ph.D.[b], Kuan-Chih Chow, Ph.D.[c], Hung-Che Huang, M.D.[d], Wen-Je Ko M.D., Ph.D.[e]

[a]Division of Thoracic surgery, Department of Surgery, China Medical University Hospital, China Meidcal University, Taichung, Taiwan;

[b]Graduate Institute of Clinical Medicine, National Taiwan University, Taipei, Taiwan;

[c]Graduate Institutes of Biomedical Sciences, National Chung Hsing University, Taichung, Taiwan;

[d]Department of Surgery, Changhua Christian Hospital,[a] Changhua, Taiwan.

[e]Department of Surgery, National Taiwan University Hospital, Taipei, Taiwan.

Address all correspondence and reprint requests to: Dr Wen-Je Ko M.D., Ph.D., Department of Surgery, National Taiwan University Hospital, Taipei, Taiwan.

Tel.: +886-2-23123456 ext 3098;

Fax:+ 886-2-23958747;

E-mail: kowj@ntu.edu.tw

or Professor Kuan-Chih Chow,

Graduate Institute of Biomedical Sciences, National Chung Hsing University, 250 Kuo-Kuang Road, Taichung 40227, Taiwan.

E-mail: kcchow@dragon.nchu.edu.tw

ABSTRACT

Primary spontaneous pneumothorax (PSP) often occurs after the rupture of small bullae or subpleural blebs in otherwise normal lungs. The underlying mechanism(s) remain unclear. The aim of this study was to identify genes potentially involved in the development of PSP. Microarray analysis was performed to identify specific gene expression patterns. Expression levels of genes identified to be significantly up or down-regulated in association with PSP were confirmed by real time polymerase chain reaction (qRT-PCR) and Western blotting. Immunohistochemistry was performed to identify lung cell types highly expressing these genes. Microarray analysis revealed that expression levels of hypoxia-inducible factor-3 alpha (HIF-3α) and caspase-8 were significantly upregulated in tissue from patients with PSP, while interferon-gamma, interleukin (IL)-6 and IL-8 were down-regulated (all $P<0.05$). These genes are related to hypoxia, apoptosis, and inflammation. HIF-3α and caspase-8 protein levels were increased in samples from patients with PSP. HIF-3α and caspase-8 were localized in mesothelial cells, alveolar type II pneumocytes and bronchoalveolar epithelial cells in samples from patients with PSP. Our findings, although obviously preliminary given the small sample size, suggest that hypoxia, inflammation, and apoptosis may play important roles in the pathogenesis of PSP.

Key words: primary spontaneous pneumothorax; gene expression; microarray; hypoxia; HIF-3α; caspase-8.

INTRODUCTION

Primary spontaneous pneumothorax (PSP) is a perplexing disease that usually occurs in young, otherwise healthy individuals, in their late teens or third decade of life without clinically apparent lung disease (1). It is defined by the presence of air in the pleural cavity and secondary lung collapse, and occurs without an obvious precipitating cause (2). The incidence of PSP is approximately 7 to 18 and 1 to 6 cases per 100,000 individuals per year in males and females respectively (3-5). Physical activity does not play a role in mediating the development of PSP, with the majority of cases of spontaneous pneumothorax occurring at rest (2,6). Smoking, however, is an important risk factor for PSP (6).

Pathophysiologically, PSP is thought to be caused by the formation of small bullae or rupture of subpleural blebs in the lung (7). However, lung parenchymal abnormalities may also be involved (6). Although the mechanism of bulla formation remains unclear, it is generally believed that the disease is caused by chronic and progressive destruction of alveolar structures at the apex of the lung, possibly due to chronic inflammation, hypoxia, oxidative stress, or an imbalance between protease and antiprotease activity (8,9). The location of the unique or diffuse sites of air leakage that lead to PSP is unknown, although a key role for distal airway inflammation due to cigarette smoking has been proposed (6). It has also been suggested that porosity of the visceral pleura is increased in patients with PSP compared to in normal individuals (6).

In this study, we used oligonucleotide microarrays (10,11) to assess differential gene expression profiles in lung tissue obtained from patients with and without PSP. Our aim was to identify genes potentially involved in mediating the underlying pathogenesis of this condition. Gene clusters were generated, and the differences in gene expression patterns were compared between the two groups of patients. Expression levels of genes found to be significantly up or down-regulated in samples from patients with PSP were determined by quantitative reverse-transcription polymerase chain reaction (qRT-PCR). Lung cell types highly expressing the specific genes were identified by immunohistochemistry.

MATERIALS AND METHODS

Lung tissue samples and initial clinical evaluation

From October 2006 to August 2007, forty consecutive patients with sporadic PSP, defined by spontaneous air accumulation in the thoracic cavity without evidence of clinical lung disease, were enrolled in the study. No patient had a family history of PSP. Wedge resection of the lung was performed by video-assisted thoracoscopic surgery. Seven lung tissue blebs from the apex of each diseased lung were collected from each patient during surgery. Lung tissue biopsies were also obtained from patients with stage I non-small cell lung carcinomas during lobectomy. These samples, used as comparative controls, were taken at least 5 cm from the tumor margin to reduce the likelihood of tumor cell invasion and

inflammation.

This study was approved by the Changhua Christian Hospital Institutional Review Board. Written informed consent was obtained from each participating individual.

RNA isolation

All samples were immediately frozen in sterile tubes by immersion in liquid nitrogen. The procedure for RNA extraction has been described previously (12). Briefly, total RNA was extracted using TRIzol® reagent (Invitrogen, Carlsbad, CA) and purified using an RNeasy Mini Kit (Qiagen, Hilden, Germany). Following extraction, RNA concentrations were quantified using an ND-1000 spectrophotometer (NanoDrop Technologies, Wilmington, DE). All isolated RNA was of high purity.

Oligonucleotide microarray

Following the synthesis of cRNA from 0.5 μg of total RNA, cRNA was amplified using a Fluorescent Linear Amplification Kit (Agilent Technologies, Santa Clara, CA) and labeled with either Cy3-CTP or Cy5-CTP fluorescent dye (Perkin-Elmer, Waltham, MA). Specifically, cRNAs from lung samples obtained from patients with PSP were labeled with Cy5, while those from control group patients were labeled with Cy3. Cy-labeled cRNA was partially fragmented into pieces of approximately 50 to 100 nucleotides long (Agilent Technologies) before being hybridized to a Whole Human Genome 4×44k oligo microarray slide (Agilent Technologies) at 60°C for 17 hours. After repeated washing, the hybridized microarrays were

scanned using a microarray scanner (Agilent Technologies) at OD_{535} for Cy3 and OD_{625} for Cy5. The scanned images were analyzed using Feature extraction software 8.1 (Agilent Technologies). The transformed data were normalized using the rank-consistency-filtering LOWESS method.

GeneSpring analysis

The transformed microarray data were analyzed using GeneSpring GX 7.3.1 (Agilent Technologies) with a defined algorithm to filter out the differentially expressed genes that had marginal flags in at least 4 of 7 samples. The differentially expressed genes were further correlated and pooled with cluster analysis and gene ontology classification was performed.

Real-time PCR

An aliquot of total RNA from each sample was used for real-time PCR. cDNA was synthesized from total RNA (5 μg) using MMLV reverse transcriptase (Promega, Madison, WI). The resultant cDNA was diluted 1:40 fold before real-time PCR analysis. Specific primer pairs were selected from the Universal ProbeLibrary™ database (http://www.exiqon.com). The primer sequences are shown in Table 1. The specificity of each primer pair was tested and confirmed using a Bioanalyzer 2100 (Agilent Technologies) for correct PCR product size. Real-time PCR was performed using a Roche LightCycler® 1.5 (Roche, Basel, Switzerland). Reaction mixtures contained 1× master mix (which included SYBR Green fluorescent dye), 3.75 μM of primer mixture, and cDNA. Each sample was run

in triplicate. Real-time PCR was carried out as follows: denaturing of the cDNA template at 95°C for 10 seconds, hybridization with primers at 60°C for 15 seconds, and DNA synthesis at 72°C for 10 seconds. In each real-time PCR run, data were automatically analyzed by the system software and an amplification plot was generated for each sample. From these plots, the crossing point (Cp) value, which indicates the beginning of the exponential amplification phase, was automatically determined by the machine-embedded software. Each PCR cycle represented a two-fold change. The fold change in relative gene expression for each sample was further calculated using the formula: 2-δδ CP (where δCp = Cp of target gene – Cp of control gene, and δδCp = δCp test sample – δCp control sample).

Western blotting

PSP lung tissue samples were suspended in lysis buffer (1% NP-40, 0.1% SDS, 0.5% sodium deoxycholate, 150 mM NaCl, 20 mM Tris-HCl pH 8, 1 mM PMSF, and protease inhibitors). A total of 100 mg of protein was separated by 12% SDS-PAGE and transferred onto PVDF membranes. Blots were blocked with 5% non-fat milk in TBS + 0.05% Tween20 (TBST) and incubated overnight at 41ºC with the primary antibodies for the following: hypoxia-inducible factor 3-alpha (HIF-3α: Abcam, Cambridge, MA), caspase-8 (Santa Cruz Biotechnology Inc., Santa Cruz, CA) or actin (Sigma: monoclonal antibody A5441 was used at 1:10000 dilution). Blots were then washed in TBST and incubated for 1 hour with the horseradish peroxidase coupled, 1:500 diluted secondary polyclonal antibody (Amersham

Biosciences, Piscataway, NJ). Blots were washed again in TBST and developed by enhanced chemiluminescence (Amersham Pharmacia Biotech Europe GmbH, Du bendorf, Switzerland).

Immunohistochemistry

Immunohistochemical staining was performed using an immunoperoxidase method as previously described (13,14). Briefly, following incubation with either HIF-3α (Abcam) or caspase-8 (Santa Cruz Biotechnology Inc.) antibodies, the immunological signals on paraffin sections were amplified using an LSAB method (Dako, Carpenteria, CA). The chromogenic reaction was visualized by peroxidase-conjugated streptavidin (Dako) and aminoethyl carbazole (Sigma). Slides were counterstained with Mayor's hematoxylin, and positive staining was identified as crimson-red granules by light microscopy.

Slide evaluation

Slide evaluation has been described previously (13,14). Four diseased areas were randomly selected for evaluation in each slide. Each slide was examined and evaluated by two independent investigators. Staining intensities were semiquantitatively scored according to the percentage of positively stained cells apparent: -, equivalent to the negative control, with less than 10% of positive cells; +, intermediate staining, positive cells were around 10% to 50%; and ++, strong staining, with more than 50% of cells positively stained.

Statistical analysis

Data are presented as median (interquartile range, IQR) for continuous variables and number (percentage) for categorical variables. Continuous and categorical variables were statistically compared by Mann-Whitney U test and Fisher's exact, respectively. Spearman's rank correlations were performed to assess correlations between the gene expression levels obtained by real-time PCR and those by oligonucleotide array. A *P*-value of 0.05 or less was defined as statistically significant. All statistical analyses were two-sided and performed using SPSS software (version 15.0, SPSS Inc., Chicago, IL).

RESULTS

Patient characteristics

Among the 44 subjects recruited for the study, 41 were males (93.2%). The median age and body mass index were 21 years (IQR: 19 to 27) and 21 kg/m^2 (IQR: 19-21). Of these, 11 (7 PSP and 4 control patients) were selected for further analysis. The clinical and demographic characteristics of these patients are summarized in Table 2.

Differentially expressed genes in patients with PSP

Among 35713 probed genes, 2841 genes were differentially expressed and had at least 2-fold changes in 5 of 7 samples from PSP patients (P <0.05). According to the cluster analysis, the 2841 genes could be categorized into three groups: Group 1, consisting of 1085 genes, Group 2, consisting of 1127 genes, and Group 3, consisting of 629 genes. Each group

was further categorized according to the function of genes identified: behavior, cell communication, response to stimulus, and cell motility. The up-regulated and down-regulated genes in Group 1 are summarized in supplementary Tables 1A and 1B. Five genes (two up-regulated: HIF-3α and caspase-8; three down-regulated: interferon-gamma [IFN- γ], interleukin [IL]-6 and IL-8) were selected from Group 1 as candidates for further characterization based on histological findings, *P*-values, and our hypothesis that hypoxia in the apex of the lung may play an important role in the development of PSP.

Candidate gene analysis

Real-time PCR was performed in an attempt to confirm the findings of microarray analysis. A significant positive correlation was apparent for IL-8 only ($P < 0.05$), with there being a borderline significant positive correlation for HIF-3α ($P = 0.052$) (Figure 1).

As real-time PCR analysis did not provide conclusive data, Western blotting was performed as another independent means to indirectly verify mRNA expression. Compared to control samples, only HIF-3α and caspase-8 showed observable differences (increases) in protein levels in six out of the seven PSP patients (Figure 2: there was insufficient sample available from one patient with PSP for Western blot analysis). Caspase-8 in particular showed marked increases in protein expression levels.

Localization of overexpressed genes as determined by immunohistochemistry

Immunohistochemical localization of HIF-3α and caspase-8 was performed in samples

obtained from patients with PSP. When expression of HIF-3α and caspase-8 was detected in consecutive sections, it indicated that HIF-3α and caspase-8 were simultaneously expressed in the same cell. HIF-3α (Figure 3) and caspase-8 (Figure 4) were identified in mesothelial cells, alveolar type II (ATII) pneumocytes and bronchoalveolar epithelial cells. Cells with enlarged cytoplasm were frequently detected in the afflicted lung tissue samples from patients with PSP, except when various degrees of alveolar deformation, cell detachment and tissue fibrosis were evident. The number of enlarged cells increased with the severity of progressive fibrosis. For severe progressive fibrosis (+ or ++), HIF-3α was detected in 80% of alveolar macrophages and 75% of both type II pneumocytes and mesothelial cells. While caspase-8 was detected in 90% of alveolar macrophages, 75% of type II pneumocytes, and 70% of mesothelial cells. Atherosclerotic pulmonary arterioles were frequently identified in nearby lung tissue, indicating that stagnated blood flow in these areas might be responsible for the decreased oxygen supply in the apical lung.

There was no evidence of blebs, fibrosis or inflammation in tissue obtained from control group patients.

DISCUSSION

The immunohistochemistry staining and Western blots performed in this study show that overexpression of HIF-3α and caspase-8 was common in patients with PSP. Identification of

HIF-3α in the nuclei of mesothelial and ATII cells suggests that these tissues had been under hypoxic conditions for some period of time. The pathological resemblance of the enlarged and detached ATII cells to SARS virus-infected pneumocytes (15), in which air exchange and oxygen supply are reduced, further supports our supposition that oxygen supply in these tissues may have been diminished. Reduced exhalation of air and a weakened pleural lining of the diseased air sac are potential contributors to the formation of subpleural blebs or bullae in PSP (8,16).

In response to oxygen deprivation, cells rapidly inhibit any energy-consuming bioactivities, preventing the initiation of sudden cell death, and simultaneously activate a transcription response that is principally mediated by HIF to ensure survival (17). HIF-1 is a transcriptional complex that consists of a heterodimer of HIF-1α and HIF-1β that binds to hypoxia-responsive elements (HRE). HIF-1β is a product of the aryl-hydrocarbon receptor (AhR) nuclear translocator (ARNT) gene that is constitutively expressed when oxygen supply is ample. Under these conditions, HIF-1α is labile. These proteins contain a basic helix-loop-helix, a Per-AhR/ARNT-Sim homology sequence (18), and N-terminal and C-terminal transactivation domains (19). Hypoxia increases HIF-1α protein stability by reducing hydroxylation of the protein, blocking its interaction with the von Hippel-Lindau protein and hence inhibiting proteasome degradation of HIF-1α.

Three types of HIF-α subunits have been identified: HIF-1α, HIF-2α and HIF-3α. Like

HIF-1α and -2α, HIF-3α dimerizes with ARNT/HIF-1β and translocates to the nuclei of hypoxic cells to bind with HRE (19). HIF-3α probably plays an important role in repressing hypoxia-related gene expression. In the case of PSP, cells in the afflicted area might not be able to respond adequately to prevent the initiation of cell death in the face of continuous oxygen deficiency (17).

We found that gene expression of caspase-8 was up-regulated in lung tissue samples obtained from patients with PSP, and that expression of this protease was localized to bronchoalveolar epithelial, mesothelial and AT II cells. Caspase-8 is a downstream effector of apoptosis-related effectors, e.g., tumor necrosis factor (TNF) and Fas. Fas, as a member of the TNF/nerve growth factor receptor family, is the receptor of the Fas ligand (FasL) (20,21). It has been demonstrated that mice deficient in Fas or FasL have lesser degrees of acute lung injury compared to wild type mice when challenged with lung immunoglobulin G immune complex deposition (22). This suggests that epithelial apoptosis induced by Fas/FasL may contribute to acute lung injury.

This study has a number of limitations that warrant mention. The major limitation is the small number of samples analyzed, which severely the limited the power of statistical analysis. We do note however, that even though real-time PCR and Western verification analysis could not be considered conclusive, three potential candidates (HIF-3α, caspase-8, and IL-8) were identified as possible mediators of PSP. These findings should be viewed as

preliminary. Future larger scale studies are warranted to confirm and extend the findings presented herein. We also acknowledge that the control samples used in the present study were not obtained from normal/healthy individuals. Although biopsies were taken well away from tumors in these patients, it is possible that expression of the genes assessed may have been influenced by patient condition.

In this study, we have utilized oligonucleotide microarray, real-time PCR and immunohistochemical methods in an attempt to identify potential candidate genes differentially regulated in patients with PSP. We found evidence that a number hypoxia-, apoptosis- and inflammation-related genes were differentially expressed upon microarray analysis, i.e., HIF-3α, caspase-8, IFN-γ, IL-6 and IL-8. Even though the expression data determined by microarray were not conclusively validated by real-time PCR, immunohistochemical staining indicated that HIF-3α and caspase-8 were highly expressed in various cell types in the apex of the lung. Future *in vivo* studies are needed to confirm and extend these findings and determine the stage at which expression changes become biologically significant and whether these changes might be of prognostic significance. We speculate that chronic hypoxia and hypoxia-induced apoptosis in the apex of the lung could be responsible for provoking local tissue responses and inflammation, which may indirectly induce apoptosis of bronchoepithelial, AT II and mesothelial cells. This would lead to alveolar sac and interstitial pleural lining structural damage, which may underlie the

formation of blebs and bullae in PSP.

DECLARATION OF INTEREST

The authors report no conflicts of interest. The authors alone are responsible for the content and writing of the paper.

ACKNOWLEDGMENTS

This study was supported by a grant from the foundation of Changhua Christian Hospital (#96-CCH-IRP-18), Taiwan.

REFERENCES

1. Noppen M. Management of primary spontaneous pneumothorax. Curr Opin Pulm Med 2003;9:272-275.

2. Weissberg D, Refaely Y. Pneumothorax: experience with 1,199 patients. Chest 2000;117:1279-1285.

3. Melton LJ, III, Hepper NG, Offord KP. Incidence of spontaneous pneumothorax in Olmsted County, Minnesota: 1950 to 1974. Am Rev Respir Dis 1979;120:1379-1382.

4. Morimoto T, Shimbo T, Noguchi Y, Koyama H, Sasaki Y, Nishiwaki K, Fukui T. Effects of timing of thoracoscopic surgery for primary spontaneous pneumothorax on prognosis and costs. Am J Surg 2004;187:767-774.

5. Gupta D, Hansell A, Nichols T, Duong T, Ayres JG, Strachan D. Epidemiology of pneumothorax in England. Thorax 2000;55:666-671.

6. Tschopp JM, Rami-Porta R, Noppen M, Astoul P. Management of spontaneous pneumothorax: state of the art. Eur Respir J 2006;28:637-650.

7. Ayed AK. Suction versus water seal after thoracoscopy for primary spontaneous pneumothorax: prospective randomized study. Ann Thorac Surg 2003;75:1593-1596.

8. Sahn SA, Heffner JE. Spontaneous pneumothorax. N Engl J Med 2000;342:868-874.

9. Noppen M, Baumann MH. Pathogenesis and treatment of primary spontaneous pneumothorax: an overview. Respiration 2003;70:431-438.

10. Hansel NN, Hilmer SC, Georas SN, Cope LM, Guo J, Irizarry RA, Diette GB. Oligonucleotide-microarray analysis of peripheral-blood lymphocytes in severe asthma. J Lab Clin Med 2005;145:263-274.

11. Dallas PB, Gottardo NG, Firth MJ, Beesley AH, Hoffmann K, Terry PA, Freitas JR, Boag JM, Cummings AJ, Kees UR. Gene expression levels assessed by oligonucleotide microarray analysis and quantitative real-time RT-PCR -- how well do they correlate? BMC Genomics 2005;6:59.

12. Provenzano M, Mocellin S. Complementary techniques: validation of gene expression data by quantitative real time PCR. Adv Exp Med Biol 2007;593:66-73.

13. Mocellin S, Rossi CR, Pilati P, Nitti D, Marincola FM. Quantitative real-time PCR: a powerful ally in cancer research. Trends Mol Med 2003;9:189-195.

14. Chen JT, Lin TS, Chow KC, Huang HH, Chiou SH, Chiang SF, Chen HC, Chuang TL, Lin TY, Chen CY. Cigarette smoking induces overexpression of hepatocyte growth factor in type II pneumocytes and lung cancer cells. Am J Respir Cell Mol Biol 2006;34:264-273.

15. Chow KC, Hsiao CH, Lin TY, Chen CL, Chiou SH. Detection of severe acute respiratory syndrome-associated coronavirus in pneumocytes of the lung. Am J Clin Pathol 2004;121:574-580.

16. Matute-Bello G, Winn RK, Jonas M, Chi EY, Martin TR, Liles WC. Fas (CD95) induces alveolar epithelial cell apoptosis in vivo: implications for acute pulmonary inflammation. Am J Pathol 2001;158:153-161.

17. Liu L, Cash TP, Jones RG, Keith B, Thompson CB, Simon MC. Hypoxia-induced energy stress regulates mRNA translation and cell growth. Mol Cell 2006;21:521-531.

18. Kikuchi Y, Ohsawa S, Mimura J, Ema M, Takasaki C, Sogawa K, Fujii-Kuriyama Y. Heterodimers of bHLH-PAS protein fragments derived from AhR, AhRR, and Arnt prepared by co-expression in Escherichia coli: characterization of their DNA binding activity and preparation of a DNA complex. J Biochem 2003;134:83-90.

19. Hara S, Hamada J, Kobayashi C, Kondo Y, Imura N. Expression and characterization of hypoxia-inducible factor (HIF)-3alpha in human kidney: suppression of HIF-mediated gene expression by HIF-3alpha. Biochem Biophys Res Commun 2001;287:808-813.

20. Nagata S. Apoptosis by death factor. Cell 1997;88:355-365.

21. Strand S, Hofmann WJ, Hug H, Muller M, Otto G, Strand D, Mariani SM, Stremmel W,

Krammer PH, Galle PR. Lymphocyte apoptosis induced by CD95 (APO-1/Fas) ligand-expressing tumor cells--a mechanism of immune evasion? Nat Med 1996;2:1361-1366.

22. Lu Q, Harrington EO, Rounds S. Apoptosis and lung injury. Keio J Med 2005;54:184-189.

FIGURE LEGENDS

Figure 1. Correlation between the gene expression fold-change alterations as determined by real-time polymerase chain reaction (RT-PCR) and microarray for 7 patients. Spearman's rank correlation was used. * Statistically significant, P<0.05.

Figure 2. Western blot detection of hypoxia-inducible factor-3α (HIF-3α), caspase-8 and β-actin in lung samples obtained from six patients with primary spontaneous pneumothorax and four control group patients.

Figure 3. Immunohistochemical localization of hypoxia-inducible factor-3α (HIF-3α) in lung tissue samples obtained from patients with primary spontaneous pneumothorax. HIF-3α expression is apparent in the representative slides shown: (A) blebs and mesothelial cells (indicated by arrows, magnification ×200); (B) aggregated alveolar type II pneumocytes in the fibrotic region (indicated by arrows, magnification ×200); (C) regenerated alveolar type II pneumocytes in thickened air sacs (indicated by arrows, magnification ×200); and (D) bronchoalveolar epithelial cells (indicated by arrows, magnification ×100).

Figure 4. Immunohistochemical localization of caspase-8 in lung tissue samples obtained from patients with primary spontaneous pneumothorax. Caspase-8 expression is apparent in

the representative slides shown: (A) mesothelial cells (magnification ×100); (B) enlarged image of (A), mesothelial cells (indicated by arrows, magnification ×400); (C) alveolar type II pneumocytes (indicated by arrows, original magnification ×200); and (D) bronchoalveolar epithelial cells (indicated by arrows, magnification ×100).

Table 1. Primer sequences used for real-time polymerase chain reaction.

Gene		Primer
HIF-3α	Sense	5'-TCTTAGCCCCATTTACCCCGTTTG-3'
	Antisense	5'-TTCCCTAGCCCAGCACAATTCC-3'
Caspase-8	Sense	5'-AAGGTGCTACCATCGTGAGAG-3'
	Antisense	5'-TTTCTGCTGAAGTCCATCTTTTT-3'
IFN-γ	Sense	5'-GGAAAGAGGAGAGTGACAGAAAA-3'
	Antisense	5'-TTGGATGCTCTGGTCATCTTTA-3'
IL-8	Sense	5'-AGACAGCAGAGCACACAAGC-3'
	Antisense	5'-ATGGTTCCTTCCGGTGGT-3'
IL-6	Sense	5'-TTCTCCACAAGCGCCTTC-3'
	Antisense	5'-AGCAGGCAACACCAGGAG-3'

HIF: hypoxia-inducible factor; IFN: interferon; IL: interleukin.

Table 2. Clinical characteristics of patients with primary spontaneous pneumothorax (PSP) and control patients.

Characteristic	**Control[#] (n=4)**	**PSP (n=7)**	***P*-value[1]**
Age (years) [2]	39.5 (34.0, 41.0)	17.0 (17.0, 24.0)	0.006*
Gender [3]			
Male	3 (75.0)	6 (85.7)	1.000
Female	1 (25.0)	1 (14.3)	
Height (cm) [2]	168.0 (162.5, 172.0)	175.0 (170.0, 178.0)	0.042*
Body weight (kg) [2]	64.0 (55.0, 70.0)	64.0 (58.0, 65.0)	0.788
Body mass index (kg/m^2) [2]	21.9 (20.8, 23.7)	19.6 (18.5, 22.5)	0.073
Surgery duration (minutes)	-	84.0 (65.0, 107.0)	-
Hospital stay (days)	-	6.0 (3.0, 7.0)	-
Smoker [3]	2 (50.0)	2 (28.6)	0.576
Side involved [3]			
Right	1 (25.0)	2 (28.6)	
Left	3 (75.0)	4 (57.1)	0.701
Bilateral	0 (0.0)	1 (14.3)	
Surgical indications			
None	-	0 (0.0)	
Ipsilateral recurrence	-	5 (71.4)	-
Persistent air leakage	-	0 (0.0)	
Contralateral recurrence	-	1 (14.3)	-
Hemopneumothorax	-	1 (14.3)	-
Bleb presence			
Single bleb	-	3 (42.9)	-

Multiple blebs	-	4 (57.1)	-

Data are presented as median (inter-quartile range) for continuous variables and number (percentage) for categorical variables.

[#] Control patients had stage I non-small cell lung carcinomas.

[1] Data were compared [2]Mann-Whiney U test or [3]Fisher's exact test.

* Indicates a statistically significant difference, $P<0.05$.

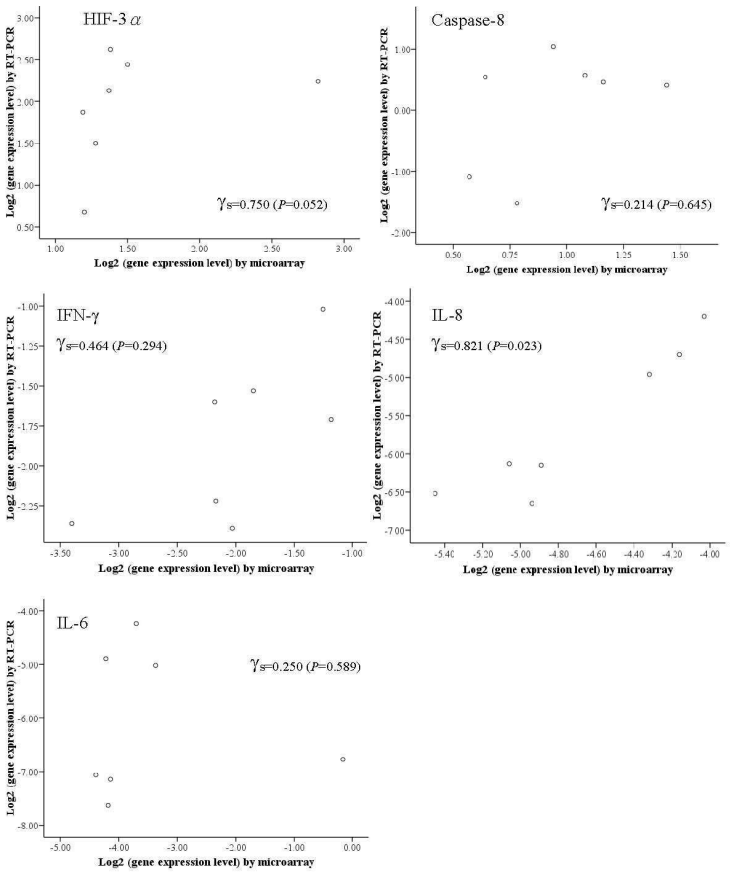

Correlation between the gene expression fold-change alterations as determined by real-time polymerase chain reaction (RT-PCR) and microarray for 7 patients. Spearman's rank correlation was used. * Statistically significant, P<0.05.
210x297mm (174 x 167 DPI)

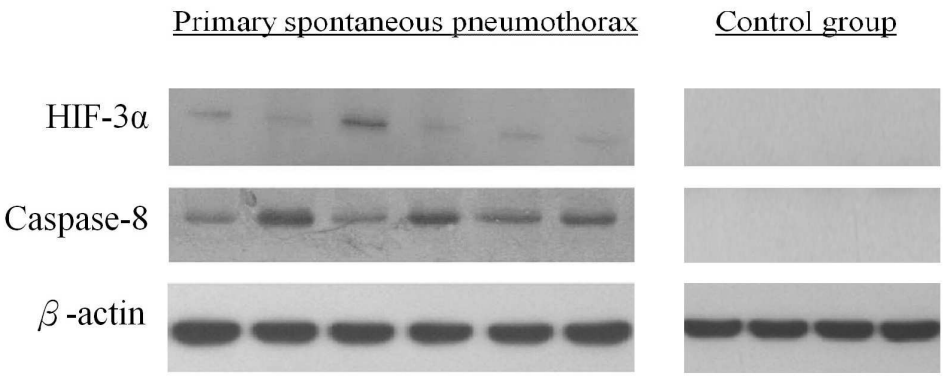

Western blot detection of hypoxia-inducible factor-3α (HIF-3α), caspase-8 and β-actin in lung samples obtained from six patients with primary spontaneous pneumothorax and four control group patients.
442x250mm (96 x 96 DPI)

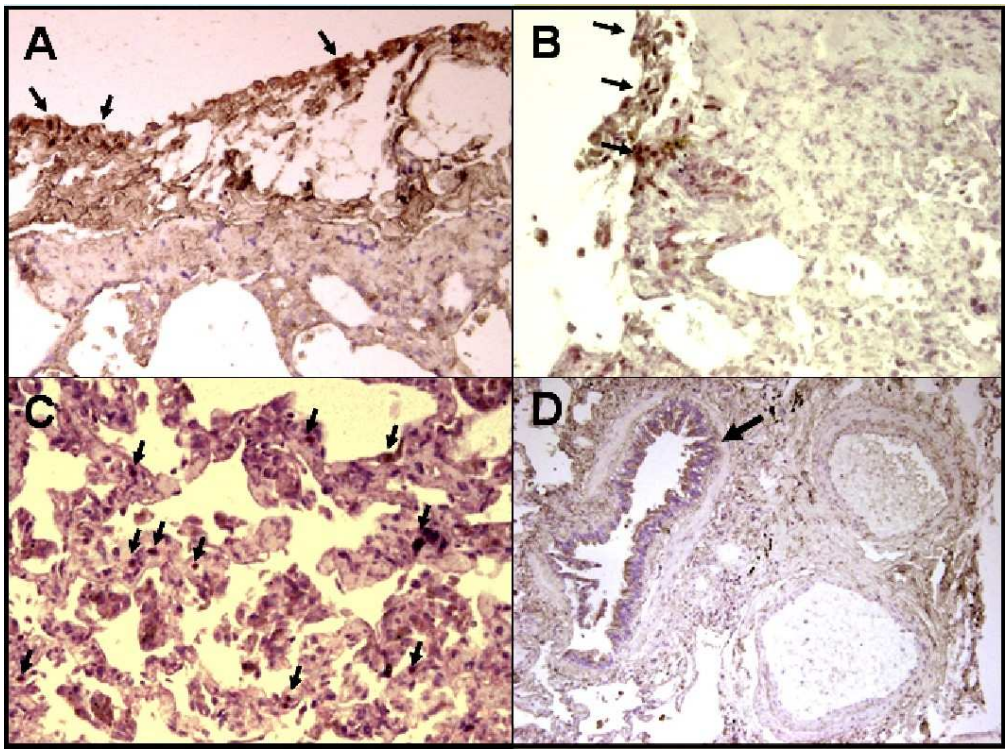

Immunohistochemical localization of hypoxia-inducible factor-3α (HIF-3α) in lung tissue samples obtained from patients with primary spontaneous pneumothorax. HIF-3α expression is apparent in the representative slides shown: (A) blebs and mesothelial cells (indicated by arrows, magnification x200); (B) aggregated alveolar type II pneumocytes in the fibrotic region (indicated by arrows, magnification x200); (C) regenerated alveolar type II pneumocytes in thickened air sacs (indicated by arrows, magnification x200); and (D) bronchoalveolar epithelial cells (indicated by arrows, magnification x100).
280x208mm (96 x 96 DPI)

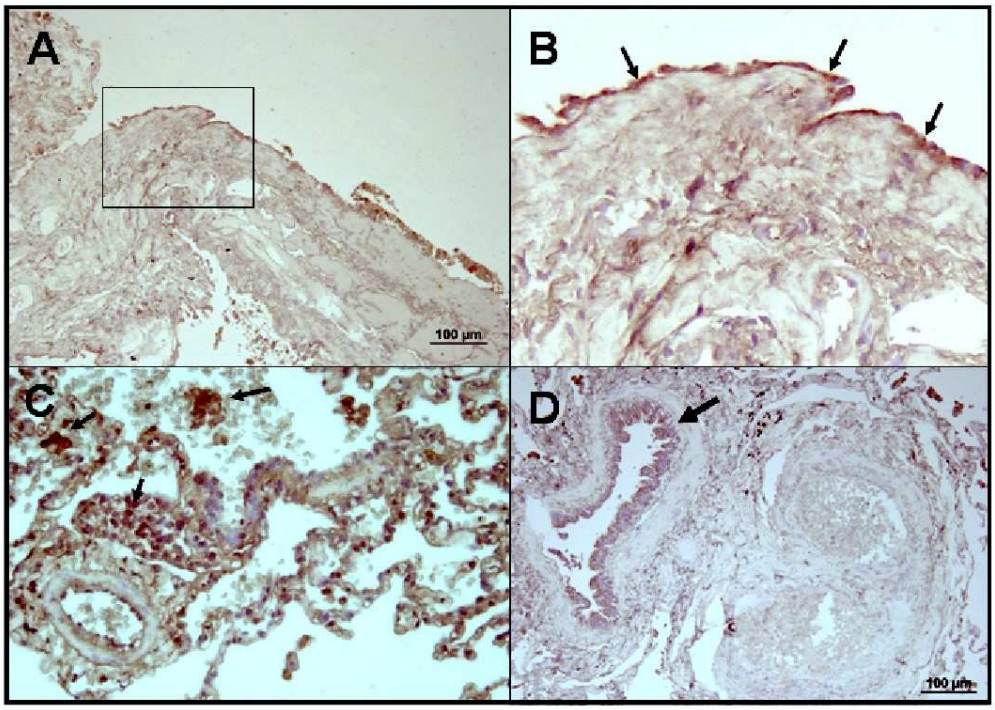

Immunohistochemical localization of caspase-8 in lung tissue samples obtained from patients with primary spontaneous pneumothorax. Caspase-8 expression is apparent in the representative slides shown: (A) mesothelial cells (magnification x100); (B) enlarged image of (A), mesothelial cells (indicated by arrows, magnification x400); (C) alveolar type II pneumocytes (indicated by arrows, original magnification x200); and (D) bronchoalveolar epithelial cells (indicated by arrows, magnification x100).
281x202mm (96 x 96 DPI)

Supplementary Table 1A: Up-regulated genes associated with the primary spontaneous pneumothorax (S.D., standard deviation)

Category	Gene ID	Description	Gene symbol	Expression Fold	S.D.
Behavior	AK026695	paxillin	PXN	2.88	0.69
	NM_000618	insulin-like growth factor 1 (somatomedin C)	IGF1	2.70	2.60
	AL133642	Enah/Vasp-like	EVL	2.31	1.50
	NM_032966	Burkitt lymphoma receptor 1, GTP binding protein (chemokine (C-X-C motif) receptor 5)	BLR1	2.18	2.66
	NM_000701	ATPase, Na+/K+ transporting, alpha 1 polypeptide	ATP1A1	2.14	0.64
	NM_000582	secreted phosphoprotein 1 (osteopontin, bone sialoprotein I, early T-lymphocyte activation 1)	SPP1	2.11	1.79
	NM_000426	laminin, alpha 2 (merosin, congenital muscular dystrophy)	LAMA2	2.08	0.87
	NM_000618	insulin-like growth factor 1 (somatomedin C)	IGF1	1.83	1.80
	AK128645	syndecan binding protein (syntenin)	SDCBP	3.01	0.54
	NM_212482	fibronectin 1	FN1	1.93	0.64
	NM_000442	platelet/endothelial cell adhesion molecule (CD31 antigen)	PECAM1	1.87	0.60
	NM_001897	chondroitin sulfate proteoglycan 4 (melanoma-associated)	CSPG4	1.71	0.64
	NM_002314	LIM domain kinase 1	LIMK1	5.28	7.53
	NM_012431	sema domain, immunoglobulin domain (Ig), short basic domain, secreted, (semaphorin) 3E	SEMA3E	2.60	1.43
	NM_001144	autocrine motility factor receptor	AMFR	1.96	1.00
	NM_001138	agouti related protein homolog (mouse)	AGRP	1.92	1.30
	NM_033181	cannabinoid receptor 1 (brain)	CNR1	1.52	1.14
Cell communication	NM_006274	chemokine (C-C motif) ligand 19	CCL19	4.12	5.72
	NM_018489	ash1 (absent, small, or homeotic)-like (Drosophila)	ASH1L	3.88	0.81
	NM_004799	zinc finger, FYVE domain containing 9	ZFYVE9	3.48	2.78
	NM_004369	collagen, type VI, alpha 3	COL6A3	3.47	2.16
	NM_013402	fatty acid desaturase 1	FADS1	3.42	1.29
	NM_000923	phosphodiesterase 4C, cAMP-specific (phosphodiesterase E1 dunce homolog, Drosophila)	PDE4C	2.95	0.65
	NM_152794	**hypoxia inducible factor 3, alpha subunit**	**HIF3A**	**2.93**	**1.22**
	NM_032023	Ras association (RalGDS/AF-6) domain family 4	RASSF4	2.84	1.26
	NM_000440	phosphodiesterase 6A, cGMP-specific, rod, alpha	PDE6A	2.76	1.16
	AK126851	ankyrin 3, node of Ranvier (ankyrin G)	ANK3	2.64	1.04

	NM_005654	nuclear receptor subfamily 2, group F, member 1	NR2F1	2.55	0.99
	NM_022740	homeodomain interacting protein kinase 2	HIPK2	2.53	0.85
	NM_006419	chemokine (C-X-C motif) ligand 13 (B-cell chemoattractant)	CXCL13	2.49	3.24
	NM_181745	G protein-coupled receptor 120	GPR120	2.42	1.16
	NM_033050	succinate receptor 1	SUCNR1	2.27	0.60
	AK098502	chromosome 9 open reading frame 39	C9orf39	2.25	0.42
	NM_001106	activin A receptor, type IIB	ACVR2B	2.24	0.65
	NM_005188	Cas-Br-M (murine) ecotropic retroviral transforming sequence	CBL	2.23	0.35
	NM_006015	AT rich interactive domain 1A (SWI- like)	ARID1A	2.22	0.40
	NM_016577	RAB6B, member RAS oncogene family	RAB6B	2.21	1.61
	NM_004443	EPH receptor B3	EPHB3	2.19	0.82
	NM_032966	Burkitt lymphoma receptor 1, GTP binding protein (chemokine (C-X-C motif) receptor 5)	BLR1	2.18	2.66
	NM_021097	solute carrier family 8 (sodium/calcium exchanger), member 1	SLC8A1	2.18	0.59
	NM_133631	roundabout, axon guidance receptor, homolog 1 (Drosophila)	ROBO1	2.15	0.46
	NM_148968	tumor necrosis factor receptor superfamily, member 25	TNFRSF25	2.13	0.50
	NM_170662	Cas-Br-M (murine) ecotropic retroviral transforming sequence b	CBLB	2.12	0.57
	NM_000582	secreted phosphoprotein 1 (osteopontin, bone sialoprotein I, early T-lymphocyte activation 1)	SPP1	2.11	1.79
	AK098194	discoidin, CUB and LCCL domain containing 1	DCBLD1	2.09	0.36
	NM_000426	laminin, alpha 2 (merosin, congenital muscular dystrophy)	LAMA2	2.08	0.87
	NM_001770	CD19 antigen	CD19	2.05	0.90
	NM_032023	Ras association (RalGDS/AF-6) domain family 4	RASSF4	2.05	0.57
	NM_000208	insulin receptor	INSR	1.98	1.04
	NM_199040	nudix (nucleoside diphosphate linked moiety X)-type motif 4	NUDT4	1.97	0.36
	NM_033356	**caspase 8, apoptosis-related cysteine protease**	**CASP8**	**1.97**	**0.47**
	NM_005900	SMAD, mothers against DPP homolog 1 (Drosophila)	SMAD1	1.96	0.75
	NM_021110	collagen, type XIV, alpha 1 (undulin)	COL14A1	1.88	1.76
	NM_000647	chemokine (C-C motif) receptor 2	CCR2	1.87	0.70
	NM_006613	GRB2-related adaptor protein	GRAP	1.87	0.72
	NM_032246	ring finger and KH domain containing 3	RKHD3	1.87	0.65

	NM_023940	RAS-like, family 11, member B	RASL11B	1.86	1.37
	NM_004385	chondroitin sulfate proteoglycan 2 (versican)	CSPG2	1.82	0.65
	NM_002609	platelet-derived growth factor receptor, beta polypeptide	PDGFRB	1.79	0.89
	NM_052884	sialic acid binding Ig-like lectin 11	SIGLEC11	1.78	0.91
	NM_004796	neurexin 3	NRXN3	1.76	0.77
	NM_000887	integrin, alpha X (antigen CD11C (p150), alpha polypeptide)	ITGAX	1.74	1.90
	NM_020182	transmembrane, prostate androgen induced RNA	TMEPAI	1.71	0.52
	L12350	thrombospondin 2	THBS2	1.67	1.35
	NM_002562	purinergic receptor P2X, ligand-gated ion channel, 7	P2RX7	1.66	0.86
	NM_013231	fibronectin leucine rich transmembrane protein 2	FLRT2	1.65	0.83
	NM_001129	AE binding protein 1	AEBP1	1.65	0.95
	NM_032457	BH-protocadherin (brain-heart)	PCDH7	1.56	0.57
	NM_013231	fibronectin leucine rich transmembrane protein 2	FLRT2	1.56	0.91
	NM_021110	collagen, type XIV, alpha 1 (undulin)	COL14A1	1.56	0.86
	NM_004933	cadherin 15, M-cadherin (myotubule)	CDH15	1.51	1.26
	NM_005849	immunoglobulin superfamily, member 6	IGSF6	1.44	0.83
	NM_004172	solute carrier family 1 (glial high affinity glutamate transporter), member 3	SLC1A3	1.36	0.96
	NM_000867	5-hydroxytryptamine (serotonin) receptor 2B	HTR2B	1.35	1.18
	NM_001953	endothelial cell growth factor 1 (platelet-derived)	ECGF1	1.26	0.75
	NM_001295	chemokine (C-C motif) receptor 1	CCR1	1.25	0.77
	NM_003247	thrombospondin 2	THBS2	1.17	0.99
	NM_000095	cartilage oligomeric matrix protein	COMP	1.16	2.02
	NM_002589	BH-protocadherin (brain-heart)	PCDH7	1.09	1.37
	NM_012445	spondin 2, extracellular matrix protein	SPON2	1.08	1.03
	NM_002314	LIM domain kinase 1	LIMK1	5.28	7.53
	NM_012431	sema domain, immunoglobulin domain (Ig), short basic domain, secreted, (semaphorin) 3E	SEMA3E	2.60	1.43
	NM_001144	autocrine motility factor receptor	AMFR	1.96	1.00
	NM_001138	agouti related protein homolog (mouse)	AGRP	1.92	1.30
	NM_033181	cannabinoid receptor 1 (brain)	CNR1	1.52	1.14
Response to stimulus	NM_006274	chemokine (C-C motif) ligand 19	CCL19	4.12	5.72
	NM_013402	fatty acid desaturase 1	FADS1	3.42	1.29
	NM_000440	phosphodiesterase 6A, cGMP-specific, rod, alpha	PDE6A	2.76	1.16
	NM_006419	chemokine (C-X-C motif) ligand 13 (B-cell chemoattractant)	CXCL13	2.49	3.24
	NM_000608	orosomucoid 2	ORM2	2.36	1.58

	NM_000607	orosomucoid 1	ORM1	2.33	1.91
	BC034271	Fanconi anemia, complementation group C	FANCC	2.33	0.47
	NM_005143	haptoglobin	HP	2.30	0.54
	NM_000104	cytochrome P450, family 1, subfamily B, polypeptide 1	CYP1B1	2.22	2.77
	NM_006107	cisplatin resistance-associated overexpressed protein	CROP	2.21	0.63
	NM_133631	roundabout, axon guidance receptor, homolog 1 (Drosophila)	ROBO1	2.15	0.46
	NM_148968	tumor necrosis factor receptor superfamily, member 25	TNFRSF25	2.13	0.50
	NM_000582	secreted phosphoprotein 1 (osteopontin, bone sialoprotein I, early T-lymphocyte activation 1)	SPP1	2.11	1.79
	NM_001770	CD19 antigen	CD19	2.05	0.90
	AK128423	cold inducible RNA binding protein	CIRBP	2.03	1.20
	NM_000821	gamma-glutamyl carboxylase	GGCX	1.98	0.31
	NM_007237	SP140 nuclear body protein	SP140	1.88	0.45
	NM_000647	chemokine (C-C motif) receptor 2	CCR2	1.87	0.70
	NM_018242	hypothetical protein FLJ10847	FLJ10847	1.87	0.48
	NM_183040	dystrobrevin binding protein 1	DTNBP1	1.84	0.53
	BC009496, XM_056455	Melanoma associated gene	D2S448	1.81	0.57
	NM_000397	cytochrome b-245, beta polypeptide (chronic granulomatous disease)	CYBB	1.56	0.73
	NM_005849	immunoglobulin superfamily, member 6	IGSF6	1.44	0.83
	NM_001953	endothelial cell growth factor 1 (platelet-derived)	ECGF1	1.26	0.75
	NM_001295	chemokine (C-C motif) receptor 1	CCR1	1.25	0.77
	NM_006569	cell growth regulator with EF hand domain 1	CGREF1	1.18	1.10
	NM_012445	spondin 2, extracellular matrix protein	SPON2	1.08	1.03
	NM_002345	lumican	LUM	1.07	0.77
	NM_032966	Burkitt lymphoma receptor 1, GTP binding protein (chemokine (C-X-C motif) receptor 5)	BLR1	2.18	2.66
	NM_000582	secreted phosphoprotein 1 (osteopontin, bone sialoprotein I, early T-lymphocyte activation 1)	SPP1	2.11	1.79
	NM_000426	laminin, alpha 2 (merosin, congenital muscular dystrophy)	LAMA2	2.08	0.87

Supplementary Table 1B: Down-regulated genes associated with the primary spontaneous pneumothorax (S.D., standard deviation)

Category	Gene ID	Description	Gene symbol	Expression Fold	S.D.
Cell communication	NM_001003683	phosphodiesterase 1A, calmodulin-dependent	PDE1A	0.80	0.80
	NM_000728	calcitonin-related polypeptide, beta	CALCB	0.76	0.56
	NM_005248	Gardner-Rasheed feline sarcoma viral (v-fgr) oncogene homolog	FGR	0.72	0.39
	NM_002436	membrane protein, palmitoylated 1, 55kDa	MPP1	0.63	0.20
	NM_005613	regulator of G-protein signalling 4	RGS4	0.62	0.38
	NM_005856	receptor (calcitonin) activity modifying protein 3	RAMP3	0.61	0.27
	NM_053064	guanine nucleotide binding protein (G protein), gamma 2	GNG2	0.60	0.23
	NM_000560	CD53 antigen	CD53	0.59	0.18
	NM_152852	membrane-spanning 4-domains, subfamily A, member 6A	MS4A6A	0.59	0.16
	NM_198148	carboxypeptidase X (M14 family), member 2	CPXM2	0.59	0.37
	NM_025216	wingless-type MMTV integration site family, member 10A	WNT10A	0.58	0.17
	NM_016184	C-type lectin domain family 4, member A	CLEC4A	0.58	0.11
	NM_005739	RAS guanyl releasing protein 1 (calcium and DAG-regulated)	RASGRP1	0.58	0.18
	NM_002616	period homolog 1 (Drosophila)	PER1	0.57	0.15
	AK131525	phosphodiesterase 2A, cGMP-stimulated	PDE2A	0.56	0.15
	NM_002843	protein tyrosine phosphatase, receptor type, J	PTPRJ	0.56	0.16
	NM_004004	gap junction protein, beta 2, 26kDa (connexin 26)	GJB2	0.56	1.36
	NM_175738	RAB37, member RAS oncogene family	RAB37	0.56	0.13
	NM_005737	ADP-ribosylation factor-like 7	ARL7	0.56	0.20
	NM_021248	cadherin-like 22	CDH22	0.56	0.12
	NM_000073	CD3G antigen, gamma polypeptide (TiT3 complex)	CD3G	0.55	0.38
	NM_004001	Fc fragment of IgG, low affinity IIb, receptor (CD32)	FCGR2B	0.55	0.29
	NM_198196	CD96 antigen	CD96	0.54	0.14
	NM_006142	stratifin	SFN	0.54	0.25
	NM_000732	CD3D antigen, delta polypeptide (TiT3 complex)	CD3D	0.53	0.20
	NM_139266	signal transducer and activator of transcription 1, 91kDa	STAT1	0.53	0.16
	NM_000591	CD14 antigen	CD14	0.53	0.23
	NM_000677	adenosine A3 receptor	ADORA3	0.53	0.24
	NM_058175	collagen, type VI, alpha 2	COL6A2	0.52	0.18

	NM_000417	interleukin 2 receptor, alpha	IL2RA	0.52	0.22
	NM_000265	neutrophil cytosolic factor 1 (47kDa, chronic granulomatous disease, autosomal 1)	NCF1	0.52	0.46
	NM_000729	cholecystokinin	CCK	0.52	0.21
	NM_002087	granulin	GRN	0.52	0.09
	NM_001937	dermatopontin	DPT	0.52	0.33
	NM_007126	valosin-containing protein	VCP	0.52	0.12
	NM_002005	feline sarcoma oncogene	FES	0.51	0.17
	NM_006072	chemokine (C-C motif) ligand 26	CCL26	0.51	0.34
	NM_001882	corticotropin releasing hormone binding protein	CRHBP	0.50	0.21
	NM_001721	BMX non-receptor tyrosine kinase	BMX	0.50	0.16
	NM_000265	neutrophil cytosolic factor 1 (47kDa, chronic granulomatous disease, autosomal 1)	NCF1	0.49	0.47
	NM_002416	chemokine (C-X-C motif) ligand 9	CXCL9	0.48	0.43
	NM_005248	Gardner-Rasheed feline sarcoma viral (v-fgr) oncogene homolog	FGR	0.48	0.38
	NM_004895	cold autoinflammatory syndrome 1	CIAS1	0.48	0.13
	NM_002985	chemokine (C-C motif) ligand 5	CCL5	0.47	0.12
	NM_004887	chemokine (C-X-C motif) ligand 14	CXCL14	0.47	0.57
	NM_002986	chemokine (C-C motif) ligand 11	CCL11	0.46	0.10
	NM_182664	Ras association (RalGDS/AF-6) domain family 5	RASSF5	0.45	0.11
	NM_001736	complement component 5 receptor 1 (C5a ligand)	C5R1	0.45	0.21
	NM_022349	membrane-spanning 4-domains, subfamily A, member 6A	MS4A6A	0.44	0.15
	NM_197954	C-type lectin domain family 7, member A	CLEC7A	0.43	0.14
	NM_002029	formyl peptide receptor 1	FPR1	0.43	0.14
	NM_003239	transforming growth factor, beta 3	TGFB3	0.41	0.22
	NM_139013	mitogen-activated protein kinase 14	MAPK14	0.41	0.08
	NM_003881	WNT1 inducible signaling pathway protein 2	WISP2	0.41	0.26
	NM_003841	tumor necrosis factor receptor superfamily, member 10c, decoy without an intracellular domain	TNFRSF10C	0.41	0.14
	NM_016084	RAS, dexamethasone-induced 1	RASD1	0.40	0.21
	NM_006564	chemokine (C-X-C motif) receptor 6	CXCR6	0.40	0.15
	NM_003014	secreted frizzled-related protein 4	SFRP4	0.39	0.71
	NM_001005377	plasminogen activator, urokinase receptor	PLAUR	0.38	0.10
	NM_001078	vascular cell adhesion molecule 1	VCAM1	0.38	0.28

	NM_004067	chimerin (chimaerin) 2	CHN2	0.37	0.14
	NM_014999	RAB21, member RAS oncogene family	RAB21	0.36	0.06
	NM_006840	leukocyte immunoglobulin-like receptor, subfamily B (with TM and ITIM domains), member 5	LILRB5	0.36	0.26
	NM_016084	RAS, dexamethasone-induced 1	RASD1	0.36	0.25
	NM_000609	chemokine (C-X-C motif) ligand 12 (stromal cell-derived factor 1)	CXCL12	0.36	0.29
	NM_002036	Duffy blood group	FY	0.35	0.09
	NM_000631	neutrophil cytosolic factor 4, 40kDa	NCF4	0.33	0.09
	NM_003853	interleukin 18 receptor accessory protein	IL18RAP	0.32	0.07
	NM_003012	secreted frizzled-related protein 1	SFRP1	0.31	0.26
	NM_002984	chemokine (C-C motif) ligand 4	CCL4	0.31	0.15
	NM_001776	ectonucleoside triphosphate diphosphohydrolase 1	ENTPD1	0.30	0.08
	NM_000576	interleukin 1, beta	IL1B	0.29	0.13
	NM_016388	T cell receptor interacting molecule	TCRIM	0.29	0.11
	NM_000619	**interferon, gamma**	**IFNG**	**0.28**	**0.08**
	NM_004951	Epstein-Barr virus induced gene 2 (lymphocyte-specific G protein-coupled receptor)	EBI2	0.26	0.08
	NM_002927	regulator of G-protein signalling 13	RGS13	0.23	0.20
	NM_016232	interleukin 1 receptor-like 1	IL1RL1	0.23	0.32
	NM_000710	bradykinin receptor B1	BDKRB1	0.22	0.10
	NM_004591	chemokine (C-C motif) ligand 20	CCL20	0.22	0.09
	NM_001937	dermatopontin	DPT	0.21	0.13
	NM_000230	leptin (obesity homolog, mouse)	LEP	0.21	0.07
	NM_020530	oncostatin M	OSM	0.21	0.06
	NM_006273	chemokine (C-C motif) ligand 7	CCL7	0.21	0.19
	NM_006564	chemokine (C-X-C motif) receptor 6	CXCR6	0.19	0.06
	NM_005408	chemokine (C-C motif) ligand 13	CCL13	0.19	0.09
	NM_005408	chemokine (C-C motif) ligand 13	CCL13	0.18	0.07
	NM_153615	Ral-GDS related protein Rgr	RGR	0.17	0.06
	NM_002178	insulin-like growth factor binding protein 6	IGFBP6	0.17	0.09
	NM_002965	S100 calcium binding protein A9 (calgranulin B)	S100A9	0.16	0.07
	NM_000655	selectin L (lymphocyte adhesion molecule 1)	SELL	0.11	0.03
	NM_000584	**interleukin 8**	**IL8**	**0.04**	**0.01**
Response to stimulus	NM_006864	leukocyte immunoglobulin-like receptor, subfamily B (with TM and ITIM domains), member 3	LILRB3	0.88	0.70

	NM_005084	phospholipase A2, group VII (platelet-activating factor acetylhydrolase, plasma)	PLA2G7	0.78	0.92
	NM_005248	Gardner-Rasheed feline sarcoma viral (v-fgr) oncogene homolog	FGR	0.72	0.39
	NM_052942	guanylate binding protein 5	GBP5	0.67	0.34
	NM_172369	complement component 1, q subcomponent, gamma polypeptide	C1QG	0.61	0.21
	BC034142	immunoglobulin kappa variable 1-5	IGKV1-5	0.60	0.31
	NM_000560	CD53 antigen	CD53	0.59	0.18
	NM_003465	chitinase 1 (chitotriosidase)	CHIT1	0.59	0.80
	NM_002000	Fc fragment of IgA, receptor for	FCAR	0.59	0.22
	NM_016184	C-type lectin domain family 4, member A	CLEC4A	0.58	0.11
	BC063385	T cell receptor alpha locus	TRA@	0.57	0.17
	NM_006272	S100 calcium binding protein, beta (neural)	S100B	0.55	0.22
	NM_006398	ubiquitin D	UBD	0.55	0.39
	NM_005516	major histocompatibility complex, class I, E	HLA-E	0.55	0.15
	NM_004001	Fc fragment of IgG, low affinity IIb, receptor (CD32)	FCGR2B	0.55	0.29
	NM_198196	CD96 antigen	CD96	0.54	0.14
	NM_006110	CD2 antigen (cytoplasmic tail) binding protein 2	CD2BP2	0.53	0.09
	NM_004159	proteasome (prosome, macropain) subunit, beta type, 8 (large multifunctional protease 7)	PSMB8	0.53	0.10
	NM_139266	signal transducer and activator of transcription 1, 91kDa	STAT1	0.53	0.16
	NM_000591	CD14 antigen	CD14	0.53	0.23
	NM_000677	adenosine A3 receptor	ADORA3	0.53	0.24
	NM_000417	interleukin 2 receptor, alpha	IL2RA	0.52	0.22
	NM_000265	neutrophil cytosolic factor 1 (47kDa, chronic granulomatous disease, autosomal 1)	NCF1	0.52	0.46
	NM_005514	major histocompatibility complex, class I, B	HLA-B	0.52	0.09
	NM_007126	valosin-containing protein	VCP	0.52	0.12
	NM_006072	chemokine (C-C motif) ligand 26	CCL26	0.51	0.34
	BC073764	immunoglobulin kappa constant	IGKC	0.50	0.26
	NM_001637	acyloxyacyl hydrolase (neutrophil)	AOAH	0.50	0.11
	NM_006866	leukocyte immunoglobulin-like receptor, subfamily A (with TM domain), member 2	LILRA2	0.49	0.15
	NM_182549	major histocompatibility complex, class II, DQ beta 2	HLA-DQB2	0.49	0.13
	NM_020992	PDZ and LIM domain 1 (elfin)	PDLIM1	0.49	0.08

	NM_000265	neutrophil cytosolic factor 1 (47kDa, chronic granulomatous disease, autosomal 1)	NCF1	0.49	0.47
	NM_002416	chemokine (C-X-C motif) ligand 9	CXCL9	0.48	0.43
	NM_005248	Gardner-Rasheed feline sarcoma viral (v-fgr) oncogene homolog	FGR	0.48	0.38
	NM_004895	cold autoinflammatory syndrome 1	CIAS1	0.48	0.13
	NM_006144	granzyme A (granzyme 1, cytotoxic T-lymphocyte-associated serine esterase 3)	GZMA	0.47	0.16
	NM_002985	chemokine (C-C motif) ligand 5	CCL5	0.47	0.12
	NM_001778	CD48 antigen (B-cell membrane protein)	CD48	0.47	0.19
	NM_000636	superoxide dismutase 2, mitochondrial	SOD2	0.47	0.28
	NM_004887	chemokine (C-X-C motif) ligand 14	CXCL14	0.47	0.57
	NM_006399	basic leucine zipper transcription factor, ATF-like	BATF	0.46	0.24
	BX161420	immunoglobulin heavy constant mu	IGHM	0.46	0.12
	NM_003650	cystatin F (leukocystatin)	CST7	0.46	0.09
	NM_002800	proteasome (prosome, macropain) subunit, beta type, 9 (large multifunctional protease 2)	PSMB9	0.46	0.12
	NM_005041	perforin 1 (pore forming protein)	PRF1	0.46	0.27
	NM_002986	chemokine (C-C motif) ligand 11	CCL11	0.46	0.10
	NM_006037	histone deacetylase 4	HDAC4	0.45	0.16
	NM_001736	complement component 5 receptor 1 (C5a ligand)	C5R1	0.45	0.21
	NM_197954	C-type lectin domain family 7, member A	CLEC7A	0.43	0.14
	NM_021139	UDP glycosyltransferase 2 family, polypeptide B4	UGT2B4	0.43	0.50
	NM_002029	formyl peptide receptor 1	FPR1	0.43	0.14
	NM_000716	complement component 4 binding protein, beta	C4BPB	0.43	0.22
	NM_002621	properdin P factor, complement	PFC	0.43	0.09
	NM_000239	lysozyme (renal amyloidosis)	LYZ	0.43	0.25
	NM_001140	arachidonate 15-lipoxygenase	ALOX15	0.42	0.26
	M20432	major histocompatibility complex, class II, DQ beta 1	HLA-DQB1	0.41	0.21
	NM_139013	mitogen-activated protein kinase 14	MAPK14	0.41	0.08
	NM_001004349	FLJ45422 protein	FLJ45422	0.39	0.16
	NM_002934	ribonuclease, RNase A family, 2 (liver, eosinophil-derived neurotoxin)	RNASE2	0.39	0.14
	NM_000129	coagulation factor XIII, A1 polypeptide	F13A1	0.39	0.28
	NM_003226	trefoil factor 3 (intestinal)	TFF3	0.38	0.16

	NM_001005377	plasminogen activator, urokinase receptor	PLAUR	0.38	0.10
	NM_000331	serum amyloid A1	SAA1	0.36	0.38
	NM_006840	leukocyte immunoglobulin-like receptor, subfamily B (with TM and ITIM domains), member 5	LILRB5	0.36	0.26
	NM_000609	chemokine (C-X-C motif) ligand 12 (stromal cell-derived factor 1)	CXCL12	0.36	0.29
	NM_001911	cathepsin G	CTSG	0.35	0.24
	NM_021822	apolipoprotein B mRNA editing enzyme, catalytic polypeptide-like 3G	APOBEC3G	0.35	0.08
	NM_001453	forkhead box C1	FOXC1	0.34	0.13
	NM_000631	neutrophil cytosolic factor 4, 40kDa	NCF4	0.33	0.09
	NM_003853	interleukin 18 receptor accessory protein	IL18RAP	0.32	0.07
	NM_005384	nuclear factor, interleukin 3 regulated	NFIL3	0.32	0.12
	NM_002984	chemokine (C-C motif) ligand 4	CCL4	0.31	0.15
	NM_001776	ectonucleoside triphosphate diphosphohydrolase 1	ENTPD1	0.30	0.08
	NM_000576	interleukin 1, beta	IL1B	0.29	0.13
	NM_021139	UDP glycosyltransferase 2 family, polypeptide B4	UGT2B4	0.29	0.36
	NM_016388	T cell receptor interacting molecule	TCRIM	0.29	0.11
	NM_000619	interferon, gamma	IFNG	0.28	0.08
	NM_004951	Epstein-Barr virus induced gene 2 (lymphocyte-specific G protein-coupled receptor)	EBI2	0.26	0.08
	NM_000710	bradykinin receptor B1	BDKRB1	0.22	0.10
	NM_004591	chemokine (C-C motif) ligand 20	CCL20	0.22	0.09
	NM_004633	interleukin 1 receptor, type II	IL1R2	0.22	0.13
	NM_020530	oncostatin M	OSM	0.21	0.06
	NM_006273	chemokine (C-C motif) ligand 7	CCL7	0.21	0.19
	NM_005408	chemokine (C-C motif) ligand 13	CCL13	0.19	0.09
	NM_002704	pro-platelet basic protein (chemokine (C-X-C motif) ligand 7)	PPBP	0.17	0.12
	NM_002965	S100 calcium binding protein A9 (calgranulin B)	S100A9	0.16	0.07
	NM_144673	chemokine-like factor super family 2	CKLFSF2	0.14	0.07
	NM_004633	interleukin 1 receptor, type II	IL1R2	0.13	0.03
	NM_005621	S100 calcium binding protein A12 (calgranulin C)	S100A12	0.09	0.05
	NM_000600	**interleukin 6 (interferon, beta 2)**	**IL6**	**0.06**	**0.02**
Cell motility	NM_006289	talin 1	TLN1	0.58	0.11
	NM_002985	chemokine (C-C motif) ligand 5	CCL5	0.47	0.12

	NM_002029	formyl peptide receptor 1	FPR1	0.43	0.14
	NM_007074	coronin, actin binding protein, 1A	CORO1A	0.42	0.15
	NM_139013	mitogen-activated protein kinase 14	MAPK14	0.41	0.08
	NM_002984	chemokine (C-C motif) ligand 4	CCL4	0.31	0.15
	NM_006135	capping protein (actin filament) muscle Z-line, alpha 1	CAPZA1	0.30	0.14
	NM_000619	interferon, gamma	IFNG	0.28	0.08
	NM_004665	vanin 2	VNN2	0.16	0.04
	NM_000655	selectin L (lymphocyte adhesion molecule 1)	SELL	0.11	0.03

彰化基督教醫院
CHANGHUA CHRISTIAN HOSPITAL

135 Nan-Hsiao Street, Changhua 500, TAIWAN
Tel :886-4-723-8595 ext.1362
E-mail:d9065@cch.org.tw
財團法人彰化基督教醫院本會

500 彰化市南校街 135 號
電話：(04)723-8595 轉 1362
E-mail: d9065@cch.org.tw

同意臨床試驗證明書

查計畫主持人：方信元/協同主持人：林同森主持「自發性氣胸病患之微陣列及基因表現分析」新案 (060832)，經本會審查通過，特此證明。有效期限至西元 2007 年 10 月 04 日，且應接受本會之監督，同意臨床試驗證明書編號：CCH：060832

後續定期追蹤之程序及要求：

1. 期中報告：應於西元 2007 年 08 月 04 日前繳交期中報告。核准有效期限屆滿，若尚未通過期中報告追蹤審查，不得繼續試驗。
2. 結案報告：試驗完成後，應將執行情形及結果以書面報告本會核備。

人體試驗委員會
主任委員
郭守仁

西 元 2006 年 10 月 04 日

Protocol Title：Lung Tissue Gene Expression Profiling in Primary Spontaneous Pneumothorax.
Protocol No：060832
Protocol Version Date：1.0 Aug 30, 2006
Informed Consent Version Date：2.0 Sep 27, 2006
Principle Investigator(s)：Hsin-Yuan Fang
Co_Investigator(s)：Torn-Sen Lin
CCH：060832
The above study was approved by the Institutional Review Board of the Changhua Christian Hospital on Oct 04, 2006 and valid till Oct 04, 2007 and accepts the monitoring of IRB.

IRB用印：

Sincerely Yours
Shou-Jen Kuo, M.D.
Chairman
Institutional Review Board,
Changhua Christian Hospital, Taiwan

財團法人彰化基督教醫院 人體試驗委員會 Institutional Review Board 彰化市南校街135號

Oct 04, 2006

(signature, date)

本會組織與執行皆符合 ICH-GCP
The Institutional Review Board performs its functions according to written Operating procedures and complies with GCP and with the applicable regulatory requirements.